


Cathodic disbonding tests operating at large cathodic potentials for long periods need current monitoring, pH control and anode isolation

Alessandro Benedetti¹ | Filippo Castelli^{2,3} | Roberto Stifanese² |
Pierluigi Traverso² | Marco Faimali² | Andrea Bergo⁴ | Marina Delucchi³ 

¹National Research Council (CNR),
Institute of Condensed Matter Chemistry
and Technologies for Energy (ICMATE),
Genoa, Italy

²National Research Council (CNR),
Institute of Anthropic Impacts and
Sustainability in Marine Environment
(IAS), Genoa, Italy

³Department of Civil, Chemical and
Environmental Engineering, DICCA,
University of Genoa, Genoa, Italy

⁴RINA, CSM, Rome, Italy

Correspondence

Alessandro Benedetti, National Research
Council (CNR), Institute of Condensed
Matter Chemistry and Technologies for
Energy (ICMATE), Via de Marini 6,
Genoa 16149, Italy.

Email: alessandro.benedetti@cnr.it

Marina Delucchi, Department of Civil,
Chemical and Environmental
Engineering, DICCA, University of
Genoa, Via Opera Pia 15, Genoa 16145,
Italy.

Email: marina.delucchi@unige.it

Abstract

Metallic structures in service in seawater are protected by coupling cathodic protection and paints, where the former may induce disbondment of the latter. A preliminary evaluation of the cathodic disbondment risk can be made by cathodic disbondment tests (CDTs). Many CDTs use cathodic potentials as large as $E < -1400$ mV versus saturated calomel electrode (SCE) applied up to 90 days. Only two CDT protocols require contemporary anode isolation, current and pH monitoring, without its correction. These three aspects were considered to develop a hybrid CDT; it consisted of polarizing steel panels at -1500 mV versus SCE for 12 weeks. The chemical effects related to the anodic processes were investigated. A pH acidic shift was observed and was justified by the increasing current demand due to paint damage and brucite precipitation on the panels. The necessity of anode isolating glass to prevent chlorine chemical attack against the paints, potentially affecting the disbondment result, was verified by estimating the virtual chemical attack induced by free chlorine. In conclusion, current monitoring, pH control and anode isolation are highly suggested to correctly conduct and interpret the cathodic disbondment results when CDTs requiring large electronegative potentials are applied for long periods.

KEYWORDS

brucite, cathodic disbonding test, free chlorine, pH

1 | INTRODUCTION

Coated metallic structures like pipeline and ship hulls in service in seawater are protected by cathodic polarization through sacrificial anodes or impressed currents. This procedure is usually coupled with the application of paints on metal surfaces. Studies regarding both active (cathodic polarization) and passive (paints) protecting techniques

are still being done.^[1–3] Interaction between coatings and cathodic currents can induce disbondment of the coatings due to cathodic reactions occurring at the metal-coating interface,^[4–6] where, due to highly alkaline pH in case of excessive cathodic protection, possible chemical dissolution of iron passive layers can be induced, too.^[7]

A practice adopted to evaluate the coating adhesion on metallic substrates consists in the application of cathodic

This is an open access article under the terms of the Creative Commons Attribution License, which permits use, distribution and reproduction in any medium, provided the original work is properly cited.

© 2022 The Authors. *Materials and Corrosion* published by Wiley-VCH GmbH.

disbondment tests (CDTs) where a cathodic polarization is imposed in controlled conditions for a determined time period. These laboratory tests are not intended to mimic real scenarios predicting in-service behaviours; rather, they provide a preliminary assessment of the coating resistance against cathodic disbondment, acting as a quality control too.^[8] The aim is to obtain the damage acceleration of paints applied on steel panels, according to polarization modes, standard techniques and surrounding parameters.^[6,9] The first CDT protocol appeared in 1969 with the publication of the standard ASTM G8, in which an artificial defect was introduced to simulate the damaged areas of a coating.^[10] Since then, many CDT protocols were edited, with different indications about coating thickness/potential/polarization time/solution/temperature^[11]; in Table 1 are summarized the main features of the most used standards that are considered in the literature.

EN ISO 15711 refers to general structures immersed in seawater, while MSC.215(82) is specifically addressed to water ballast tanks. All the other standards refer to the oil and gas sector and consider pipelines both immersed in seawater and buried.

Low-voltage tests like EN ISO 15711 are relatively closer to field conditions, but longer times are required to induce significant disbonding; on the other hand, it can be induced faster by larger cathodic potentials, as actually preferred by most of the CDT protocols (see Table 1). During the application of CDT methods, issues can arise in both the cathodic and anodic compartments. At the cathodic site, in full artificial seawater, polarizing currents can induce the precipitation of the calcareous deposit on free metal surfaces,^[12-14] which can retard the coating delamination in correspondence with the artificial defect.^[15] At the anodic site, the chlorine pollution induces the formation of active chlorine species^[16] able to provide a chemical attack with the possible acceleration of the disbonding.^[17,18] In relation to this aspect, it is worth noticing that despite this evidence 'the majority of cathodic disbondment testing data have been obtained without anode isolation'^[19]; a task still deserving consideration.^[20] It is recalled here that anode isolation consists of the placement of the anode in a glass with a porous bottom. This allows both the exchange of charged species with the solution and the contemporary delivery to the atmosphere of evolving chlorine, preventing the onset of the $\text{Cl}_2/\text{HClO}/\text{ClO}^-$ oxidative chemistry in solution.

To the best of our knowledge, in the CDT area, two authors investigated the effect on paints determined by the chlorine produced at the anode. Al-Borno et al.^[21] applied -1500 mV versus saturated calomel electrode

(SCE) for 28 days to verify whether different methods of anode isolation may affect the chemical attack over paints. It was concluded that, irrespectively of isolating techniques, anode working without isolation was decisive *per se* in determining heavier disbonding results. Betz et al.^[8] evaluated the single NaClO effect during the application of the ISO 21809-2 procedure. Regarding pH, Table 1 shows that all the CDT protocols require no acidic shift of the pH. Considering this parameter, the work of Guan et al.^[19] is worth of interest, presenting 58 responses to a questionnaire sent to coating suppliers, coating applicators and independent testing laboratories. The questions worth of interest are the following:

- Do you completely change the electrolyte periodically for long-term tests? Yes, 63%; no 37%.
- Do you monitor the pH of the electrolyte during testing? Yes, 17%; no 83%.
- Do you adjust the pH of the test electrolyte adding a pH buffer solution? Yes, 13%; no 87%.

The important indication is that pH is scarcely controlled, that is, monitored and adjusted, during CD tests.

Table 1 shows that CDT protocols adopt a generally potentiostatic polarization method, but not all of them actually require current monitoring, as it should be practised in line with Holub's et al. statement '... a good CDT Standard should specify current measuring [...] alongside the voltage specification'.^[17]

Hence, relevant aspects of the CDT application are (i) current monitoring is useful, albeit not always required; (ii) anode isolation deserves careful attention; (iii) pH monitoring is generally required, but scarcely considered. Among the protocols listed in Table 1, only ASTM G95 and NACE TM0115-2015 require contemporary anode isolation, current monitoring and pH monitoring (but not its correction, as other CDTs recommend). In particular, about the NACE TM0115-2015 standard, a recent paper^[22] reviews how it was developed as a 'universal CDT method' by the NACE Technical Committee TG470 following the results of the NACE International Technical Exchange Group TEG 349X, which was formed to 'investigate the difference in test parameters selected in eight international standards as well as their influences on the disbondment results'. Actually, although in Xu et al.,^[22] the TM0115-2015 standard is regarded as a 'universal method covering all the parameters in the CD', the possibility of modifying existing tests for particular needs or applications is regarded.

TABLE 1 Main features of the most common CDT methods

Method	E (mV vs. SCE)	Solution	Time (days)	T (°C)	pH	I	Cl ₂ control (anode isolating glass)
AS3862 ^a	Intensiostatic 3 mA	3% NaCl	Multiple choices	Multiple choices	-	3 mA	Required
ASTM G8 ^a	-1420	ASW	30-60-90	23	>10	-	-
ASTM G42	-1420	ASW	60	23	>10	To be monitored	/
ASTM G95	-2920	ASW	90	23	To be monitored	To be monitored	Required
BS EN 10289	-1500	3% NaCl	2	60	6-9	/	/
			28	23			
BS EN 12068	-1420	3% NaCl	28	25	/	/	/
CSA Z-245 ^a	-1500	3% NaCl	28	20	7	-	/
EN ISO 15711	-1050	ASW	182	23	6	/	/
ISO 21809-1	-1500	3% NaCl	28	23	6-9	/	/
	-3500		1	65			
MSC.215(82)	Zn anode	Cyclic immersion in ASW or NSW	182	35	/	/	/
NACE TM0115-2015	-1420	3% NaCl	28	20-25	To be monitored once a week	To be monitored	Required

Note: (-) the parameter is not mentioned in the literature reference that speaks about the standard; (/) the parameter is not mentioned in the standard.

Abbreviations: ASW, artificial seawater; NSW, natural seawater; -, the parameter is not mentioned in the literature that speaks about the standard; /, the parameter is not mentioned in the standard; SCE, saturated calomel electrode.

^aStandard reviewed in literature not directly.

On these bases, a new hybrid CDT method was derived from EN ISO 15711 and BS 10289 standards: the testing time of the first standard was reduced to 3 months, and, the more cathodic potential of the second standard, -1500 mV versus SCE, was selected. During the CD test, polarization current was monitored, pH was controlled and the anode, generally isolated, was occasionally made to work free to evaluate the possible virtual chemical attack. The aim of monitoring these parameters was to investigate effects related to anodic processes occurring on CDT featured by large cathodic potentials applied for long periods and to interpret the obtained results.

2 | EXPERIMENTAL

Table 2 resumes the details of the two standard protocols inspiring the hybrid CDT procedure and the selected parameters identifying it.

As shown in Figure 1, the paints were applied on 12 carbon steel panels, $100 \times 150 \times 4$ mm each, homogeneously distributed along the wall of a 70 cm diameter tank filled with 100 L of artificial seawater (sodium chloride 23 g L^{-1} , magnesium chloride hexahydrate 9.8 g L^{-1} , sodium sulphate decahydrate 8.9 g L^{-1} and calcium chloride 1.2 g L^{-1}).

A 6 mm diameter circular defect was drilled in the centre of each panel. Pt anode was placed inside an isolating glass. The potential was applied with a

Gamry Potentiostat/Galvanostat/ZRA Interface 1010E and held at -1500 mV versus SCE. Both the anode and the reference electrode were placed in the centre of the tank, determining a nominal radial distance of 35 cm between the anode and cathodes.

During the CD test, the polarization current, I , and the pH were monitored in presence of the anode isolating glass. In particular, only in correspondence of the 2nd, 6th and 12th weeks the anode isolating glass was removed, to collect pH and free Cl data from 10 ml solution taken at about 1 cm near the anode and near the cathode. All the measurements

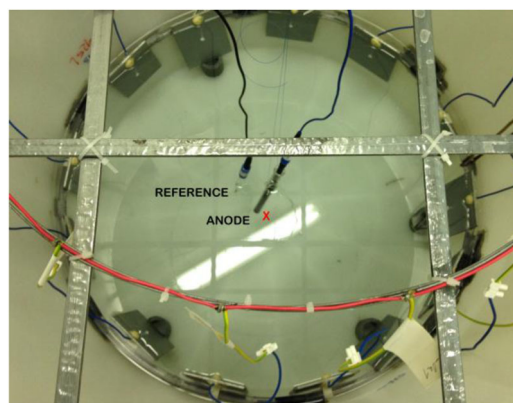


FIGURE 1 Disposal of the painted panels in the 100 L tank. The red X represents the point where the 10 ml solution was taken for the pH and free chlorine monitoring. [Color figure can be viewed at wileyonlinelibrary.com]

TABLE 2 Details of EN ISO 15711, BS 10289 and the hybrid procedure applied here

Standard parameter	EN ISO 15711	BS 10289	Hybrid procedure
Solution composition	Artificial seawater	NaCl 3%	Artificial seawater
Solution replacement (days)	≤7	/	≤7
Shape of the electrolytic cell	Tank	Rigid plastic tube	Tank
Diameter (cm)	≥70	≥0, 50	≥70
Solution volume (l)	100	≥0, 150	100
Diameter of the artificial defect on the cathode (mm)	10	10	6
Bulk pH	/	6 < pH < 9	6 < pH < 9
Test duration (weeks)	26	0.3	12
Temperature (°C)	Room	60	Room
Applied potential (mV vs. SCE)	-1050	-1500	-1500
Anode	Pt, graphite	Pt	Pt
Anode/cathode surface ratio	/	>1	<1
Anode isolating glass	/	/	Yes

Note: In bold are evidenced the parameters coming from EN ISO 15711 and BS 10289 methods composing the hybrid procedure. The anode worked isolated. Occasionally, the isolating glass was removed to allow free chlorine diffusion, aiming to the determination of the virtual chemical attack, CA_v .

lasted the time necessary to observe the pH/free Cl plateaus, always reached within 2.5 days. Thereafter, the anode was again protected and the solution was renewed adjusting the pH to 9 with NaOH 1 M. The free Cl was evaluated with DPD (*N,N*-diethyl-*p*-phenylenediamine) colorimetric method. Finally, the weight of the precipitated brucite at the end of the hybrid CDT application was determined.

A separate experiment was devoted to investigate the relationship between the brucite precipitation and pH evolution in the bulk of the solution. A carbon steel wire cathode, 2.5 mm in diameter and 225 mm in length, was statically polarised in a 0.3 L cell at $I = 10$ mA for 245 min achieving $\text{pH}(t)$ and $E(t)$ versus SCE data. The counter electrode was a Pt wire. The testing electrolytes were NaCl 3 wt.% solution versus artificial seawater. The test was performed at room temperature.

3 | RESULTS

Figure 2 reports the time evolution of the current necessary to polarize the painted panels at -1500 mV versus SCE for the whole duration of the test.

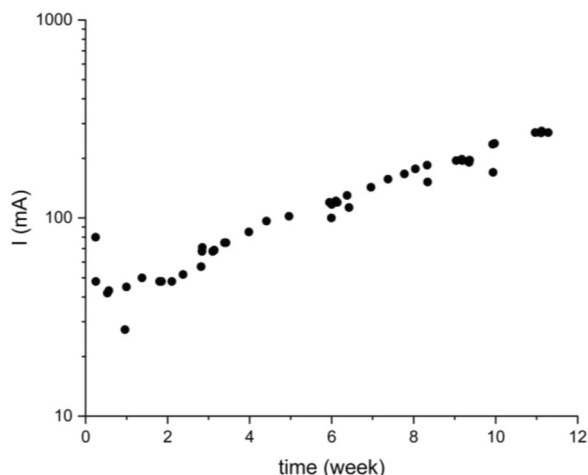


FIGURE 2 Time evolution of the current necessary to keep the painted panels polarized at -1500 mV versus SCE.

TABLE 3 pH and free chlorine, data achieved in correspondence of Weeks 2, 6, 9.5, 12

Anode isolation	Week	I (mA)	Free Cl (ppm)	pH
No	2	45	8	6.25
No	6	120	14	3.95
Yes	9.5	200	14.95	3.5
No	12	270	15	3.15

Polarization current increased from the initial value $I_0 \approx 45$ mA to the final value of 270 mA at the end of the 12 weeks period.

In Table 3 are reported the I , pH and free Cl values reached at Weeks 2, 6, 9.5 and 12. The pH after 2 weeks and the free Cl after 9.5 weeks were extrapolated.

It can be seen that current enhances, free Cl increases and pH decreases over time.

Figure 3 shows in detail the time evolution of free Cl and pH near the anode and the cathode at $I = 270$ mA, in correspondence to Week 12, just before the end of the hybrid CDT.

For free Cl, it took about 24 h to observe values lying within the same order of magnitude (i.e., in the range 1–10 ppm) near the anode and near cathode; thereafter, it took around 30 more hours to read the same value of 15 ppm near both the anode and the cathode.

Regarding pH, a rapid drop below 6 is evident, reaching values around 3. The time necessary for pH to shift from 9 to 6 near the anode, $t_{\text{pH}6}^{\text{an}}$, and near the cathode, $t_{\text{pH}6}^{\text{cat}}$, was derived from pH data at $I = 50, 120, 200, 270$ mA (in correspondence of Weeks 2, 6, 9.5 and 12) and plotted in function of I (Figure 4a). The difference between these two times, $\Delta t_{\text{pH}6} = t_{\text{pH}6}^{\text{cat}} - t_{\text{pH}6}^{\text{an}}$, is plotted as well (Figure 4b).

It can be observed that $\Delta t_{\text{pH}6}$ rapidly decreases as the current increases.

In Figure 5, as an example, the appearance of a painted panel at the end of the CDT, after 12 weeks, is presented. The areas where brucite grew are evidenced.

The brucite amount precipitated during the CDT application on all the panels was 150 g.

The relation between the brucite growth and the acidic drift was investigated with a galvanostatic test cathodically polarizing a carbon steel wire in NaCl 3% versus artificial seawater solutions (0.3 L cell, 0.5 mA cm^{-2} , 245 min).

It can be seen that the pH in the NaCl solution remained generally stable (Figure 6a), while in artificial seawater, it decreased from the initial value $\text{pH}_i \approx 8$ to the final experimental value $\text{pH}_e = 2.75$ (Figure 6c). The brucite weight measured at the end of the polarization was 0.05 g.

4 | DISCUSSION

The application of the hybrid cathodic disbonding test was characterized by the occurrence of important phenomena related to anodic processes, which were revealed by the monitoring of I , free Cl and pH. These aspects are successively discussed.

The increasing current demand (see Figure 2) is related to the increase of paint-damaged areas, which

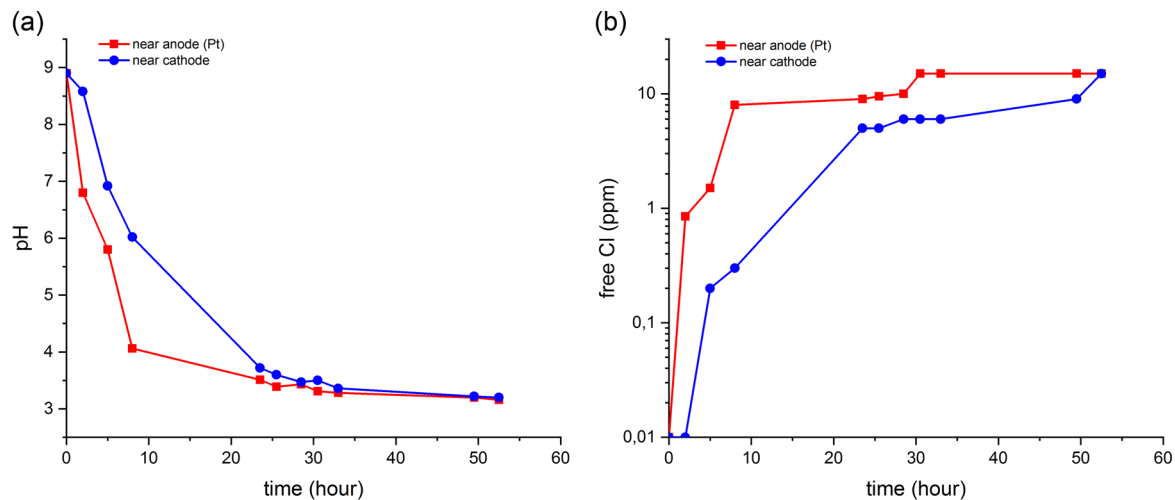


FIGURE 3 Time evolution (at $I = 270$ mA after 12 weeks) of (a) pH, (b) free Cl concentration. Data were achieved near Pt anode and near cathode, that is, one of the painted panels placed at the edge of the tank (see Figure 1). [Color figure can be viewed at wileyonlinelibrary.com]

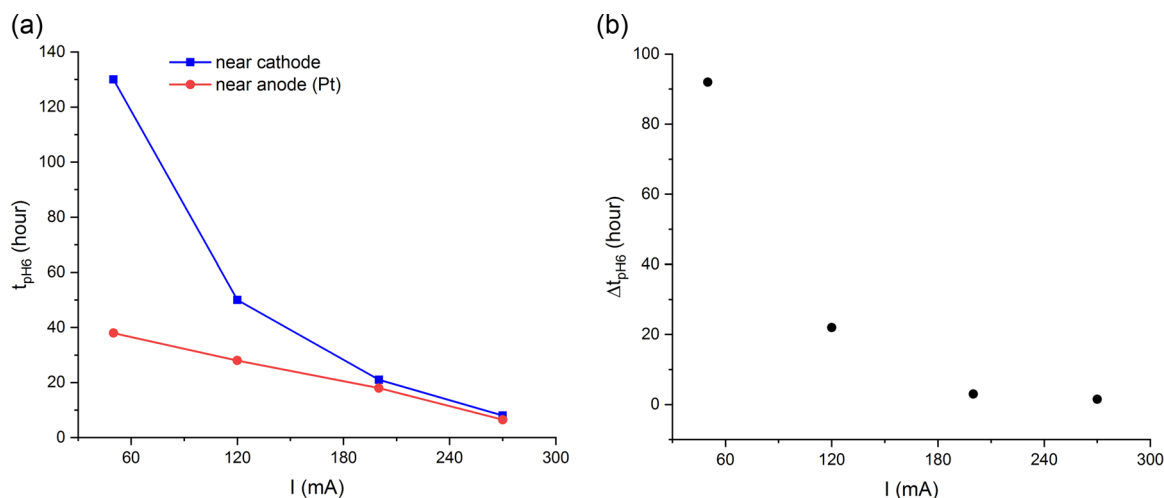


FIGURE 4 Dependence on I of (a) the time necessary to see $\text{pH} = 6$ at the anode, $t_{\text{pH}6}^{\text{an}}$ and pH at the cathode, $t_{\text{pH}6}^{\text{cat}}$. (b) difference, $\Delta t_{\text{pH}6} = t_{\text{pH}6}^{\text{cat}} - t_{\text{pH}6}^{\text{an}}$. [Color figure can be viewed at wileyonlinelibrary.com]

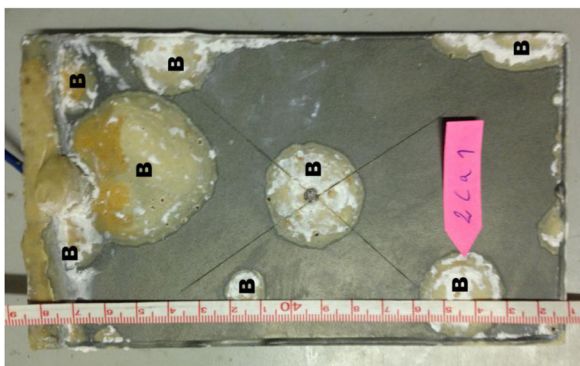


FIGURE 5 Appearance of a painted panel at the end of the hybrid CD test application (-1500 mV vs. SCE, 12 weeks, T_{room}). 'B' is the area occupied by the brucite growth.

were covered by brucite deposits appearing away from the artificial defect, too (Figure 5).

About chlorine, in real applications, its production does not threaten paints, at least away from the anodes. During CDT applications, the practice of anode isolation avoids Cl_2 delivery in the solution, potentially able to modify disbondment results,^[17] which should depend only on cathodic processes developing at the metal/paint interface. Nevertheless, as seen in Table 1, some of the cited CDT methods do not require anode isolation, in addition, noteworthy studies found in literature ascertaining the chemical effects related to anode working freely did not provide free Cl data.^[8,21]

In the present paper, to correctly apply the hybrid CDT method isolating the anode, and, contemporarily

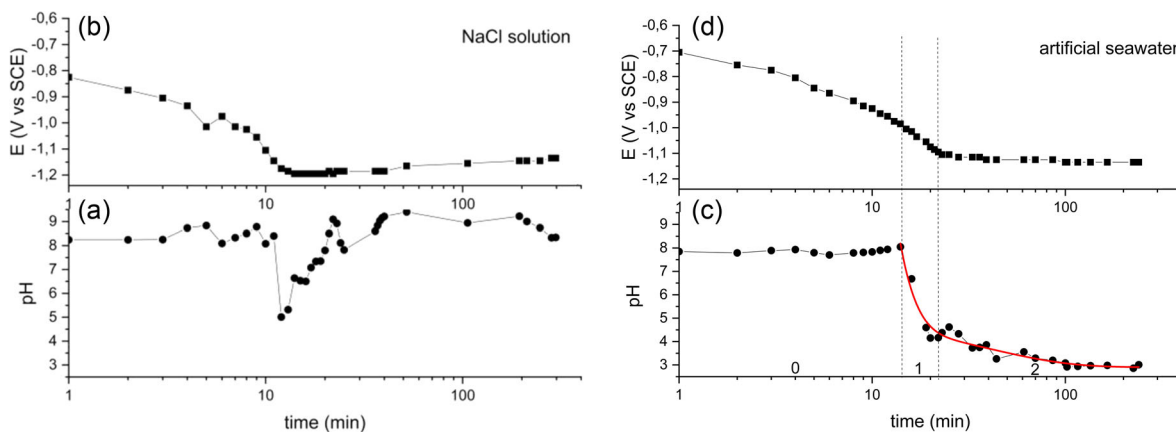


FIGURE 6 $\text{pH}(t)$ and $E(t)$ curves during galvanostatic polarization of a carbon steel cathode wire $\phi = 2.5$ mm and 20 cm^2 in NaCl solution and artificial seawater inducing brucite precipitation. Polarizations were performed imposing 0.5 mA cm^{-2} for 4.5 h at T_{room} . [Color figure can be viewed at wileyonlinelibrary.com]

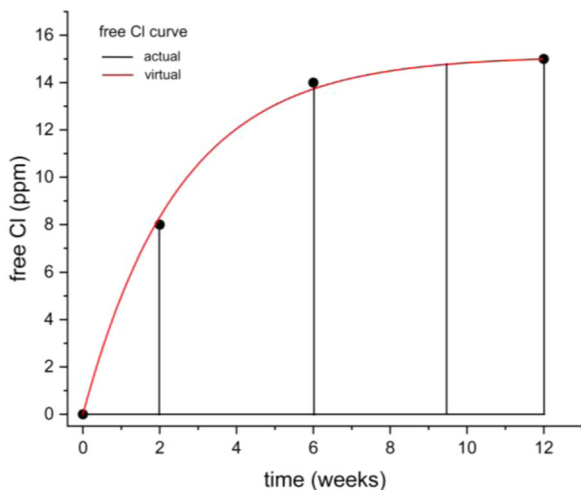


FIGURE 7 Actual free chlorine data (black curve) by which the virtual free chlorine curve, $C_v(t)$ (red curve) is derived. The integration of the latter allows obtaining the virtual chemical attack, CA_v ($\text{ppm} \times \text{h}$). [Color figure can be viewed at wileyonlinelibrary.com]

understand the free Cl impact in absence of anode isolation, the virtual chemical attack

$$CA_v = \int C_v(t) dt \quad (1)$$

was estimated, being $C_v(t)$ the virtual free Cl curve, obtained fitting the actual free Cl data reported in Table 3.

In Figure 7, the actual and virtual free Cl curves are distinguished, in particular, the area under the $C_v(t)$ curve, CA_v , represents the chemical attack to which the

painted panels would be exposed if the anode would work always as not isolated.

The CA_v parameter is inferred by the chemical treatment used in the area of filtering membranes restoration and disinfection,^[23,24] which is computed integrating the time-dependent NaClO concentration feeding the treatment^[25] with pH governing $\text{Cl}_2/\text{HClO}/\text{ClO}^-$ percentages. Here, the chemical attack is related to the free chlorine determined by the Cl_2 discharged at the anode.

By Equation (1), it is $CA_v \approx 21\,000 \text{ ppm} \times \text{h}$. By comparison, this value doubles the actual CA delivered during a 90 days experiment conducted in absence of cathodic polarization at different pH/free Cl conditions on paints for ship hulls, which felt evident damages after the exposition (data to be published). Hence, the worries about CDT data achievement without anode isolation^[19], witnessed by Song and colleagues^[8,21], are proved especially when intense cathodic potentials are applied for long times, when chemical stresses induced by anodic processes can reach noticeable extents.

Actually, even if anode isolation prevents chlorine diffusion in the solution and its use is recommended, it does not prevent pH modifications.

During the application of the hybrid CDT protocol, increasing acidification of the solution was observed. This occurrence was described as the propagation of the $\text{pH} = 6$ front from anode to cathode, whose apparent travelling speed, S , is determined as $S = 35/\Delta t_{\text{pH}6}$, being 35 cm the anode–cathode distance.

Knowing the time evolution of the current, $I(w)$ (w : week, the time unit in Figure 2) and $\Delta t_{\text{pH}6}(I)$ (see Figure 4b), combining the fit for $S(I)$ (see Equation 2) with the fit for $I(w)$ in terms of $\log [I(w)/I_0]$

(see Equation 3), the time evolution of the pH = 6 front travelling speed, $S(w)$, can be derived (see Equation 4):

$$S(I) = \frac{35 \text{ cm}}{\Delta t_{\text{pH}6}(I)} = \frac{35}{Ae^{-\frac{I}{b}} + c}, \quad (2)$$

$$\log \left[\frac{I(w)}{I_0} \right] = d + g \times w, \quad (3)$$

$$S(w) = \frac{35}{Ae^{-\frac{I_0 10^{d+g \times w}}{b}} + c}. \quad (4)$$

Being $A = 257.77 \text{ h}$, $b = 48.71 \text{ mA}$, $I_0 = 42.3 \text{ mA}$, $c = -0.238 \text{ h}$, $d = -0.0248$, $g = 0.0751 \text{ w}^{-1}$ the fitting parameters, it is $r^2 = 0.99$ for Equation (2) and $r^2 = 0.94$ for Equation (3).

The graphs of Equations (2-4) are reported in Figures 8-10 respectively.

Looking at Figure 10, it results $S = 0.42 \text{ cm h}^{-1}$ after a couple of weeks; it means that, once pH = 6 was measured near the anode, the time necessary for the pH = 6 front to travel from anode to cathode is about 3.5 days. Differently, near the end of the CD test, S resulted about 100 times faster; the practical implication for CDT management was an increase in NaOH corrections and solution renewals, facing the increasing acidification of the solution.

Acidification of the solution reflects a modification of the balance between H^+ produced at the anode and OH^- produced at the cathode. An acidic balance requires OH^- to disappear from the solution. $\text{Mg}(\text{OH})_2$ precipitation,

actually encountered during CDT, determines OH^- subtraction.

It is well known that the appliance of a cathodic potential on metals in seawater induces the precipitation of a mineral deposit made of CaCO_3 and $\text{Mg}(\text{OH})_2$: the more cathodic the potential, the larger the fraction of brucite, $\text{Mg}(\text{OH})_2$.^[12] In particular, brucite precipitation starts at $\text{pH} > 9.5$, which is met on the electrode interface cathodically polarized with $i > 0.5 \text{ mA cm}^{-2}$ and potentials more cathodic than -1100 mV versus SCE^[26]; at -1500 mV versus SCE

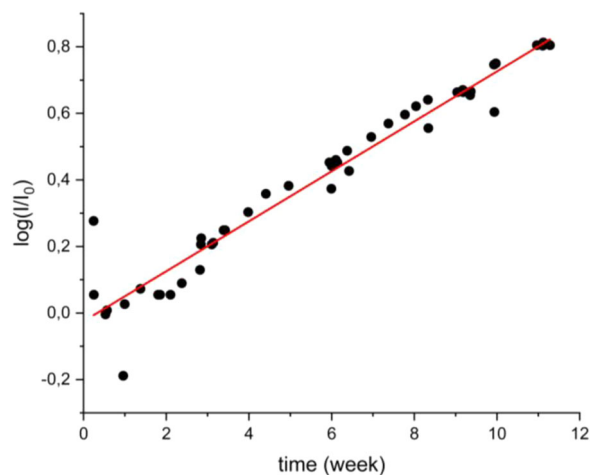


FIGURE 9 Time evolution of $\log(I/I_0)$ being I the time-dependent polarization current and I_0 the current value read after 1 week, during the application of the cathodic disbondment test (see Table 2 for details). [Color figure can be viewed at wileyonlinelibrary.com]

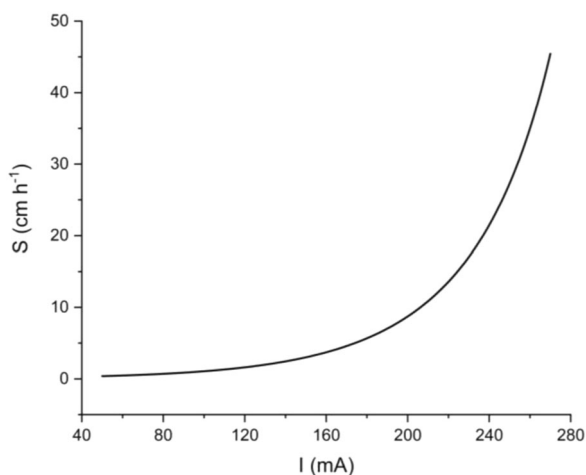


FIGURE 8 Travelling speed of S , the 'pH = 6 front', from the Pt anode to one painted panel steel (cathode) once the pH = 6 value is seen near the anode. The $S = f(I)$ curve, with I being the polarization current, results by Equation (2).

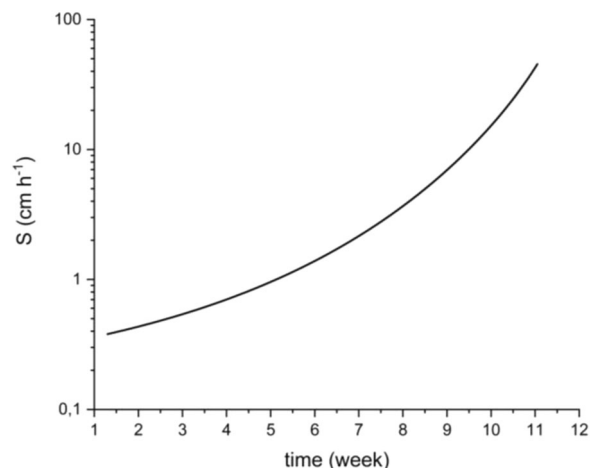
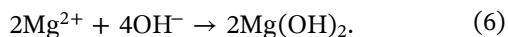
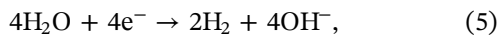


FIGURE 10 Travelling speed S of the 'pH = 6 front' from the Pt anode to cathode (one painted panel steel) in function of time (Equation 4), obtained combining Equations (2) and (3).

(the potential employed here) water reduction drives the precipitation of a mineral deposit composed of Mg(OH)₂^[14,27,28]:



OH⁻ subtraction during brucite precipitation can induce acidification due to H⁺ left in the solution, which is delivered at the anode during oxygen evolution reaction, OER:



Hence, as long as the current circulates, the acidification driven by OH⁻ storage by brucite precipitation takes place. Effectively, at the end of the hybrid CDT, the brucite weight was 150 g. This result reflects the positive balance between the precipitation due to the cathodic current flow and the dissolution due to pH < 9.5. Even if a constant dissolution rate, ranging from 10⁻⁵ to 10⁻⁷ mol m⁻² s⁻¹ at pH ~ 3 and 10⁻⁹–10⁻⁸ mol m⁻² s⁻¹ at pH ~ 8^[29–31] is considered, about 125 cm² of brucite spots distributed on the painted panels were found at the end of the hybrid CD test. Hence, the brucite growth rate overwhelmed its dissolution rate, the first depending on the current density, the second on pH.

The acidification effect determined by OH⁻ subtraction is directly proportional to the bare area of the polarized metal, as long as current densities suitable for brucite precipitation are provided. As a matter of fact, the increase of metal area exposed to the solution due to the progressive damage of the paint determined an increase of the current requirement necessary to sustain the -1500 mV versus SCE polarization potential, with current density values always suitable for brucite precipitation,^[12,32] increasing in time.

The relation between acidic shift and brucite precipitation was investigated with a galvanostatic polarization performed in NaCl 3 wt.% versus artificial seawater (see Figure 6).

The decrease of pH due to H⁺ left in the solution in relation to OH⁻ stored by brucite precipitation can be figured out with: (i) a model fitting the pH(*t*) curve in artificial seawater, (ii) computation;

- (i) the pH(*t*) curve in artificial seawater is described by three intervals. In the first interval, 0–15 min, pH ≈ 8 with *E*_{corr} decreasing from -645 to -990 mV versus SCE (Figure 6c, interval 0); it is likely related to reduction processes of iron oxides with no or

negligible brucite precipitation leaving the pH basically unmodified. In the 15–245 min period of time the pH drop is well described by a two-kinetics decay model (*r*² = 0.92), where interval 1 and interval 2 can be evidenced:

$$\text{pH}(t) = R_1 e^{-\frac{t}{\tau_1}} + R_2 e^{-\frac{t}{\tau_2}} + \text{pH}_m, \quad (8)$$

where *R*₁ = 2.8, τ₁ = 1.99 min, *R*₂ = 3.11, τ₂ = 17.02 min, pH by the model of Equation (8), pH_{*m*} = 2.26 are the fitting parameters.

In the 15–22 min interval (Figure 6c, interval 1), pH decreased rapidly (τ₁ = 1.99) and *E* shifted from -990 to -1100 mV versus SCE, in relation to the precipitation of the first brucite layer growing on the metal/solution interface. In the 22–245 min interval (Figure 6c, interval 2) pH decreased further, but at the slower rate of τ₂ = 17.02 with *E* going from -1100 to -1140 mV versus SCE, witnessing successive slower brucite growth.

- (ii) the brucite weight, *w*_b, storing OH⁻, can be computed equalling the OH⁻ moles trapped in the precipitated brucite by Reactions (5) and (6), to H⁺ moles produced at the anode by Reaction (7):

$$\left(\frac{w_b}{M_b}\right) \times n_b = \left(\frac{It}{F}\right) \times n_{\text{H}^+}, \quad (9)$$

with

- *w*_b = brucite weight; g,
- *M*_b = brucite molar weight; 58.32 g mol⁻¹,
- *n*_b = 2 OH⁻ moles in 1 brucite mole (see Reaction 6); 2 mol OH⁻/1 mol b,
- *I* = current generating OH⁻ by Reaction (5); 0.01 A,
- *F* = Faraday constant; 96 485 C mol⁻¹ e⁻,
- *t* = the time window of decreasing pH (intervals 1 and 2 in Figure 6c); 230 min × 60 s min⁻¹,
- *n*_{H⁺} = 1 mol H⁺/1 mol e⁻

By Equation (9), it results *w*_b = 0.042 g. The computed pH, pH_{*c*}, is provided by Equation (10):

$$\text{pH}_c = -\log \left[10^{-\text{pH}_i} + \frac{\left(\frac{It}{F}\right) \times n_{\text{H}^+}}{V} \right]. \quad (10)$$

Being the solution volume *V* = 0.3 L, by Equation (10) it is obtained pH_{*c*} = 2.32.

In the simple 0.3 L galvanostatic experiment, two outcomes clearly indicate that OH⁻ storage by brucite precipitation determines a pH acidic shift: (1) the

similarity between the measured and computed brucite weights (0.042 and 0.05, respectively), (2) the similarity among the experimental, modelled and computed pH ($\text{pH}_e = 2.75$, $\text{pH}_m = 2.26$, $\text{pH}_c = 2.32$).

Since in the 100 L CD test, the pH acidic shift was observed in parallel to the paint damage, the polarization current and the brucite precipitation increase, then, an OH^- storage effect by brucite precipitation is inferred. Nevertheless, since the cathode in the 100 L CD test is a more complex system (painted steel cathodes) with respect to the 0.3 L experiment (bare steel cathode), it is possible that a fraction of OH^- might be consumed in other chemical processes involving the paints.

Finally, the present work shows that I , pH and free Cl data collection allowed a wider comprehension of the involved phenomena and new insights into the CDTs, in the perspective of comparing^[33] or modifying existing CDT protocols.^[34,35]

5 | CONCLUSIONS

A hybrid cathodic disbondment test, CDT, was derived from EN ISO 15711 and BS 10289 standards and was applied to carbon steel panels painted with epoxy resin. The anode worked with the isolating glass, and it was removed a few times to estimate the virtual chemical attack related to free chlorine concentration. The polarization current was monitored and pH was controlled. The attention paid to these key parameters allowed making insights about the anodic processes, as summarized in the following:

- the estimation of the virtual chemical attack, confirms that anode isolation is necessary to avoid any additional chemical effect altering the cathodic disbonding results, which should depend only on cathodic processes at the metal/paint interface;
- in turn, the anode isolation does not allow the control of pH of the solution, which shifted acidic below the required 6–9 interval. Practically, NaOH corrections and solution renewals were adopted to keep the pH within the required range. This evidence showed that pH needs to be monitored, despite its control is generally required, but often neglected;
- the monitoring of the polarization current allowed understanding that the acidic shift of pH was related to the increasing current demand which, in turn, was connected to the paint damage and brucite precipitation at the cathodes.

Therefore, especially when CDTs require intense cathodic potentials applied for long periods, our work showed that pH monitoring is necessary to make adjustments, anode isolation is necessary to prevent chlorine oxidative pollution potentially altering CDT outcomes, and polarization current monitoring helps to improve the interpretation of the cathodic disbonding results.

ACKNOWLEDGEMENTS

The authors want to thank Prof. R. Botter for his contribution to the data collection. This study was funded in part by Italian Ministry of University and Research (Grant Nos. 2017X7Z8S3 LUBRI-SMOOTH, programme PRIN 2017). Partial financial support was received from Azienda Chimica Genovese, ACG. Open Access Funding provided by Università degli Studi di Genova within the CRUI-CARE Agreement.

CONFLICT OF INTEREST

The authors declare no conflict of interest.

DATA AVAILABILITY STATEMENT

The data that support the findings of this study are available from the corresponding author upon reasonable request.

ORCID

Marina Delucchi  <http://orcid.org/0000-0001-6640-898X>

REFERENCES

- [1] J. H. Kim, Y.-S. Kim, J.-G. Kim, *Ocean Eng* **2016**, *115*, 149.
- [2] Y.-S. Kim, S. K. Lee, J.-G. Kim, *Ocean Eng* **2018**, *163*, 476.
- [3] C. Thiel, K. Neumann, F. Ludwar, A. Rennings, J. Doose, D. Erni, *Ocean Eng* **2019**, *192*, 106560.
- [4] H. Bi, J. Sykes, *Corros. Sci.* **2011**, *53*, 3416.
- [5] Y. Da Kuang, F. Cheng, *Corros. Sci.* **2015**, *99*, 249.
- [6] S. Shreepathi, *Prog. Org. Coat.* **2016**, *90*, 438.
- [7] I. Song, D. Gervasio, J. H. Payer, *J. Appl. Electrochem.* **1996**, *26*, 1045.
- [8] M. Betz, C. Bosch, U. Smith, R. Grabowsky, P. Gronsfield, M. Bagaviev, presented at CORROSION 2012, Salt Lake City, Utah, USA, March 11-15, **2012**, 1285.
- [9] K. R. Larsen, *Mater. Perform. Magazine* **2016**, *55*, 32.
- [10] J. L. Luo, C. J. Lin, Q. Yang, S. W. Guan, *Prog. Org. Coat.* **1997**, *31*, 289.
- [11] F. Mahdavi, M. Forsyth, M. Y. J. Tan, *Prog. Org. Coat.* **2017**, *105*, 163.
- [12] C. Barchiche, C. Deslouis, D. Festy, O. Gil, P. Refait, S. Touzain, B. Tribollet, *Electrochim. Acta* **2003**, *48*, 1645.
- [13] C. Deslouis, D. Festy, O. Gil, G. Rius, S. Touzain, B. Tribollet, *Electrochim. Acta* **1998**, *43*, 1891.
- [14] C. Deslouis, D. Festy, O. Gil, V. Maillot, S. Touzain, B. Tribollet, *Electrochim. Acta* **2000**, *45*, 1837.

- [15] S. Touzain, Q. Le Thu, G. Bonnet, *Prog. Org. Coat.* **2005**, *52*, 311.
- [16] O.Ø. Knudsen, J. I. Skar presented at *CORROSION 2008*, New Orleans, Louisiana March 16–20, **2008**, paper n. 08005.
- [17] J. Holub, D. T. Wong, M. Tan, presented at *CORROSION 2007*, Nashville, Tennessee, March 11-15, **2007**, paper n. 07022.
- [18] J. H. Payer, K. M. Fink, J. J. Perdomo, R. E. Rodriguez, I. Song, B. Trautman, presented at *1st International Pipeline Conference*, Calgary, Alberta, Canada, June 9–13, **1996**, pp. 471.
- [19] S. W. Guan, J. A. Kehr, *Mater. Perform. Magazine* **2015**, *54*, 32.
- [20] B. T. A. Chang, D. Wong, presented at *CORROSION 2018*, Phoenix, Arizona, USA, April 15-19, **2018**, 11018.
- [21] A. Al-Borno, M. Brown, S. Rao, presented at *CORROSION 2008*, New Orleans, Louisiana, USA, March 16-20, **2008**, 08007.
- [22] M. Xu, C. N. C. Lam, D. Wong, E. Asselin, *Prog. Org. Coat.* **2020**, *146*, 105728.
- [23] E. Arkhangelsky, D. Kuzmenko, V. Gitis, *J. Membr. Sci.* **2007**, *305*, 176.
- [24] X. Gan, T. Lina, F. J. X. Zhang, *J. Membr. Sci.* **2021**, *640*, 119770.
- [25] P. Zhao, J. Meng, R. Zhang, B. Cao, P. Li, *Sep. Purif. Technol.* **2021**, *268*, 118671.
- [26] C. Gabrielli, G. Maurin, H. Francy-Chausson, P. Theyry, T. T. M. Tran, M. Tlili, *Desalination* **2006**, *201*, 150.
- [27] G. Salvago, S. Maffi, A. Benedetti, L. Magagnin, *Electrochim. Acta* **2004**, *50*, 169.
- [28] K. E. Mentel, W. H. Hartt, T. Y. Chen, *Corros.* **1992**, *48*, 489.
- [29] G. Jordan, W. Rammense, *Geochim. Cosmochim. Acta* **1996**, *60*, 5055.
- [30] O. S. Pokrovsky, J. Schott, *Geochim. Cosmochim. Acta* **2004**, *68*, 31.
- [31] D. A. Vermilyea, *J. Electrochem. Soc.* **1969**, *116*, 1179.
- [32] A. Benedetti, L. Bramanti, G. Tsounis, M. Faimali, G. Pavanello, S. Rossi, J. M. Gili, G. Santangelo, *Biofouling* **2011**, *27*, 799.
- [33] G. Weber, B. J. Merten, J. D. Torrey, presented at *CORROSION 2018*, Phoenix, Arizona, USA, April 15-19, **2018**, 10914.
- [34] M. Mahdavian, R. Naderi, M. Peighambari, M. Hamdipour, S. A. Haddadi, *J. Ind. Eng. Chem.* **2015**, *21*, 1167.
- [35] M. Xu, C.N.C. Lam, D. Wong, E. Asselin, *Prog. Org. Coat.* **2020**, *146*, 105728.

How to cite this article: A. Benedetti, F. Castelli, R. Stifanese, P. Traverso, M. Faimali, A. Bergo, M. Delucchi, *Mater. Corros.* **2022**, 1–11.
<https://doi.org/10.1002/maco.202213281>